The Performance of the GPSC/MSGC Hybrid Detector With Argon–Xenon Gas Mixtures

C. M. B. Monteiro, J. F. C. A. Veloso, J. M. F. dos Santos, and C. A. N. Conde

***Abstract*—The performance for X-ray spectrometry of argon–xenon gas proportional scintillation counters (GPSCs) using a CsI-coated microstrip plate in direct contact with the scintillation gas as a vacuum ultraviolet photosensor is investigated for different argon–xenon mixtures. The GPSC/microstrip gas chamber hybrid detectors filled with argon–xenon mixtures present superior performance when compared to those with pure argon and pure xenon fillings. For these mixtures, the signal amplification due to the scintillation processes and the detector energy resolution may achieve values of 15–18 and 11–10%, respectively. The best energy resolutions can be achieved for mixtures with a broad range of xenon concentration, 20–70% Xe, and for lower reduced electric fields in the scintillation region as the xenon concentration is reduced. As in pure argon or pure xenon gas-filling, the detector performance is limited by optical positive feedback resulting from additional scintillation produced in the electron avalanche processes around the microstrip plate anodes. The best energy resolutions are achieved for positive feedback gains of about 1.1.**

***Index Terms*—CsI-photocathode, gas scintillation counter, microstrip gas chamber (MSGC), X-ray.**

I. Introduction

The FEASIBILITY of detecting vacuum ultraviolet (VUV) photons using a microstrip gas chamber (MSGC) with the microstrip plate (MSP) coated with a thin layer of CsI as a photocathode operating in reflective mode was demonstrated by Zeitelhack *et al.* [1]. The potential advantages of combining a xenon gas proportional scintillation counter (GPSC) with such a MSGC as the photosensor replacement for the photomultiplier tube (PMT) was recognized [2], [3]. A significant advantage of such photosensor results from the possibility of operating the CsI-coated MSP in direct contact with the GPSC Xe-filling gas [2], with the elimination of the GPSC scintillation window. Such a GPSC/MSGC hybrid detector has been recently successfully operated [4].

This hybrid detector presents an attractive alternative to PMT-instrumented GPSCs in applications where cost, compactness, detection area, and power consumption are important. Additionally, integrated photosensors present a simple solution for operation at higher pressures than standard GPSCs. Although the energy resolution achieved with a xenon GPSC/MSGC hybrid detector (12% at 6 keV [4]) is not as good as that of photomultiplier-based GPSCs (8% at 6 keV), the performance is already better than other xenon detectors based on charge amplification, i.e., proportional counters and MSGC. The advantages gained in compactness, ruggedness, reduced power consumption, and relative insensitivity to operation in large magnetic fields [5] are in themselves desirable attributes.

The detector performance is limited by optical positive feedback resulting from the additional scintillation light produced in the charge avalanche at the MSP anodes in the absence of quenching and by the poor conversion efficiency of VUV scintillation into photoelectrons. Improvements can be obtained using MSPs with larger cathode-to-anode gap spacing and larger cathode strips [6].

Additionally, the low collection efficiency of photoelectrons emitted by the CsI photocathode in a xenon atmosphere (20 to 50% of the efficiency under vacuum for electric fields of 5 to 25 kV cm^{-1} above the photocathode surface [7]) is one of the limiting factors of the performance of the xenon hybrid detector. On the other hand, the photoelectron collection efficiency in an argon atmosphere may reach values above 90% for electric fields above 5 kV cm^{-1} [8]. However, the photoelectron collection efficiency achieved in an argon-filled hybrid detector [9] was not as high as that achieved in [8], the difference being attributed to the different energy distributions of the photoelectrons emitted by the CsI when irradiated by 185-nm light (used in [8]) and 130-nm light (the argon scintillation) [10], [11].

The improvement of the GPSC/MSGC hybrid detector performance may be achieved using argon–xenon mixtures as the filling gas. Argon-xenon mixtures may present advantages over pure argon and/or pure xenon, combining the improved collection efficiency achieved in argon with the lower mean energy to produce primary electrons, the more favorable VUV photon scintillation (172 nm), and the higher MSP charge gain achieved in xenon [9].

In this paper, we present experimental results obtained with a GPSC/MSGC hybrid detector filled with different argon–xenon mixtures. The best experimental operation conditions, scintillation amplification, and energy resolution will be investigated for each mixture.

II. Experimental System

The GPSC/MSGC hybrid detector is depicted schematically in Fig. 1 [4].

It features a 4-cm-deep absorption/drift region and a 1-cm deep scintillation region separated by a mesh grid, G1 (80-μm-diameter stainless-steel wire with 900-μm spacing). The radiation window and the focusing electrode F are maintained at

Manuscript received November 23, 2001; revised February 15, 2002. This work was supported by Project CERN/P/FIS/40112/2000. The work of J. F. C. A. Veloso was supported by Fundação para a Ciência e Tecnologia.

The authors are with the Physics Department, University of Coimbra, P-3004-516 Coimbra, Portugal (e-mail: jveloso@gian.fis.uc.pt).

Publisher Item Identifier S 0018-9499(02)06122-1.

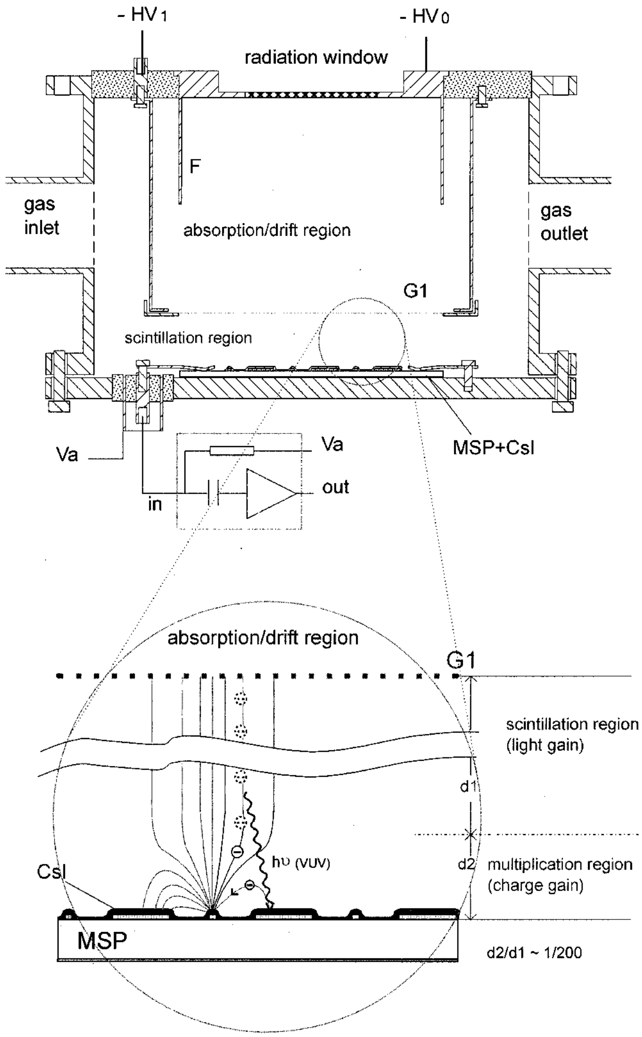

Fig. 1. Schematic of the GPSC/MSGC hybrid detector.

negative high voltage $-\mathrm{HV}_0$, while the G1-grid and its holder electrode are kept at $-\mathrm{HV}_1$. The PMT commonly used as the UV photosensor in GPSCs is substituted in this detector by a CsI-coated MSP, which is placed in direct contact with the GPSC gas-filling. The MSP is a CERN model MS-4, consisting of 10-μm anodes and 80-μm cathodes with a 200-μm pitch, fabricated of 0.2-μm-thick chromium film deposited on a 500-μm Desag D263 glass substrate. The backplane is a flat, unstructured layer of 0.1-μm chromium. The backplane and cathodes are maintained at ground potential while a positive voltage V_a is applied to all the anodes.

A 500-nm-thick and 30-mm-diameter layer of high-purity CsI was vacuum deposited onto the surface of the MSP. Special care was taken to avoid water contamination of the CsI film: the MSP was heated at temperatures of about 100 °C during 1 h before CsI evaporation; the exposing time of the CsI film to air during the transfer process was less than 10 min; and the CsI film was heated under vacuum at about 80 °C for 24 h after the CsI-covered MSP had been placed inside the detector [12]–[14].

The electric field in the drift region is determined by the voltage difference between G1 and the radiation window while the G1 voltage determines the electric field in the scintillation region. The anode strip voltage determines the MSP gain. The detector is filled with different argon–xenon mixtures at 800 Torr (106 kPa).

The ionizing radiation interacts in the absorption region and the resulting primary electron cloud drifts toward the scintillation region under the influence of a weak electric field (below the gas scintillation threshold). The electric field in the scintillation region is rather higher than in the absorption region but lower than the gas ionization threshold, so that electrons can excite but not ionize the gas atoms. Upon crossing the scintillation region toward the MSP anode strips, each electron will produce a large number of VUV photons as a result of the gas deexcitation processes. The scintillation light intensity is proportional to the number of primary electrons and, thus, to the X-ray energy. The VUV scintillation photons incident on the CsI-photocathode induce the emission of photoelectrons from the active areas, the cathode strips. The photoelectrons drift toward the anode strips, producing charge avalanches in the intense electric field, and so a large signal proportional to the number of primary electrons produced by the X-rays in the gas.

Thus, the CsI-coated MSP serves simultaneously as the GPSC collection grid for the primary electron cloud, the photosensor for the GPSC VUV scintillation, and the amplification stage for the photoelectrons. While the upper region d_1 functions as the uniform-field scintillation region of a conventional GPSC, the region d_2 (<50 μm) functions as a standard MSGC. This hybrid system functions as a GPSC rather than an MSGC [2], [4].

A 2-mm collimated 5.9-keV X-ray beam from a ^{55}Fe radioactive source, with the 6.4-keV K_β-line filtered by a chromium foil, was used to induce detector pulses. The anode pulses were preamplified with a Canberra 2006 charge-to-voltage preamplifier (sensitivity of 235 mV/10^6 ion pairs), linearly amplified with a Tennelec TC243 amplifier (8-μs peaking time constants), and pulse-height analyzed with a 1024-multichannel analyzer. For peak amplitude and energy-resolution measurements, pulse-height distributions were fitted to a Gaussian superimposed on a linear background, from which the centroid and the full-width at half-maximum were determined.

III. Experimental Results and Discussion

The presence of the CsI-coating does not compromise the operation of the MSP. Instead, it results in a reduced substrate charge built up since its semiconductive characteristics are comparable to those of the semiconducting glass substrates used for high-rate MSP applications [14], [15].

Fig. 2 presents typical pulse-height distributions obtained with the hybrid detector for a 2-mm collimated 5.9-keV X-ray beam and for different Ar–Xe mixtures. The detector biasing voltages applied in each case were those corresponding to the best performance. The spectral features include the 5.9-keV peak, the argon and/or xenon escape peaks, and the electronic noise tail in the low-energy limit. The argon K-fluorescence escape peak is negligible for xenon concentrations above 10%, while the xenon L-fluorescence escape peak is already present for xenon concentrations of 70%. The limit of the low-energy noise tail decreases with increasing xenon concentration, being about 800 eV for pure argon, around 600–500 eV for

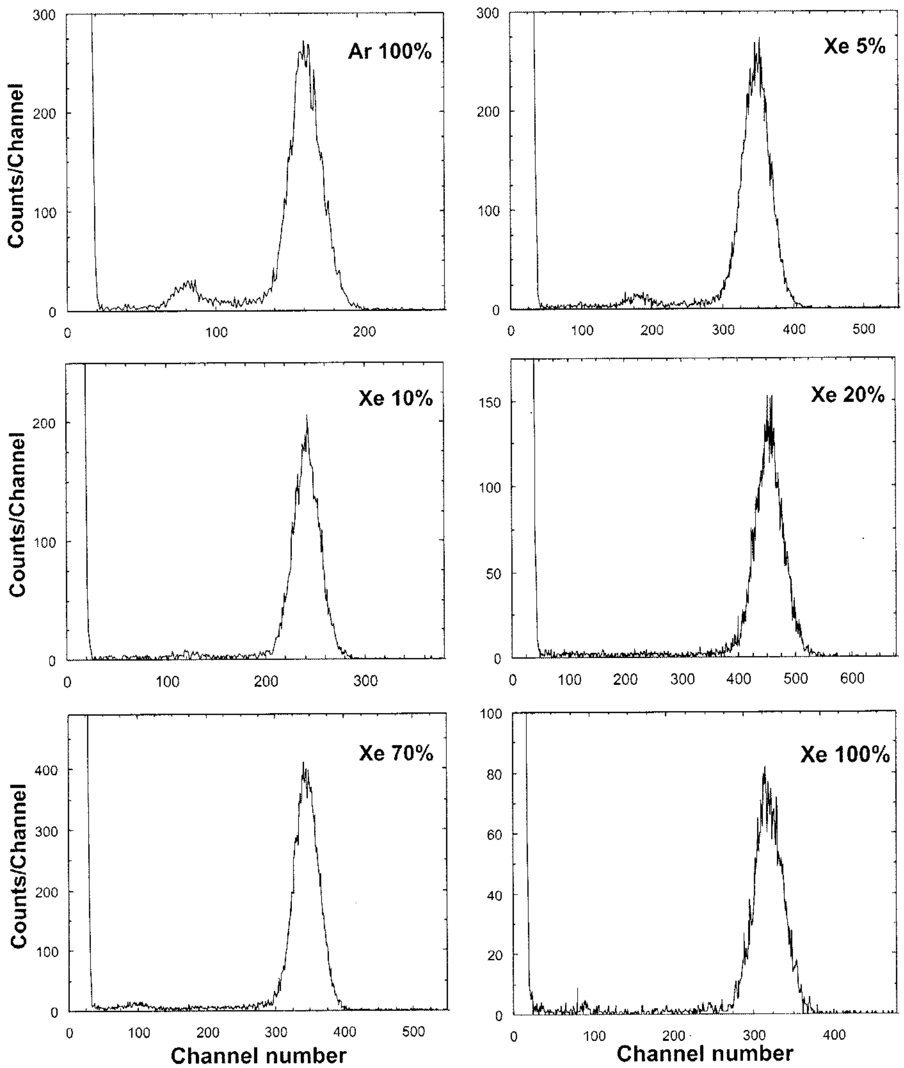

Fig. 2. Typical pulse-height distributions for 5.9-keV X-rays obtained with the GPSC/MSGC hybrid detector for different argon–xenon mixtures. The detector biasing voltages applied in each case correspond to those that deliver the best achieved performance.

xenon concentrations between 10–70%, and about 250 eV for pure xenon. In fact, this behavior could be attributed to the number of microdischarges that decrease with increasing xenon concentration.

In Fig. 3, we present the detector relative pulse amplitude as a function of the MSP anode voltage V_a for the different argon–xenon mixtures while maintaining constant the electric fields in the drift and scintillation regions. Exponential functions (solid lines) are superimposed on the experimental results for comparison. As seen, the MSP gain depicts the characteristic exponential variation of the charge avalanche processes at the MSP anodes, until a faster increase departs from the initial behavior, due to optical positive feedback resulting from additional scintillation produced in the electron avalanche processes, which becomes significant for high V_a voltages.

The optical positive feedback limits the MSP maximum gain by limiting V_a, since positive feedback introduces additional statistical fluctuations that lead to a degradation of the detector energy resolution. In Fig. 4, we depict the detector energy res-

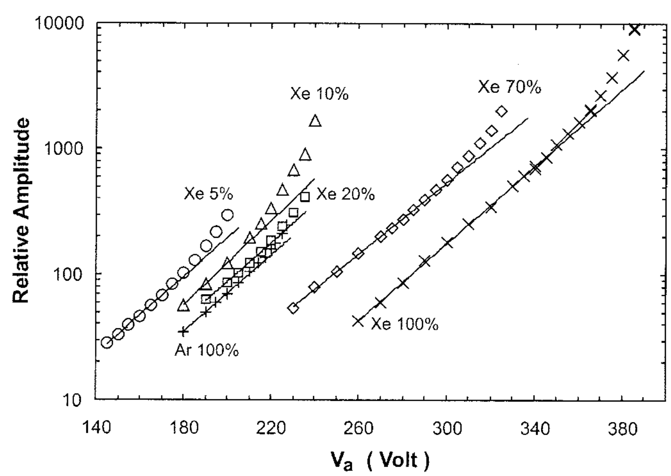

Fig. 3. Detector relative pulse amplitude as a function of the anode-to-cathode strip voltage V_a for constant reduced electric fields in the drift and scintillation regions and for the different argon–xenon mixture fillings. Exponential functions (solid lines) are superimposed to the experimental results for comparison.

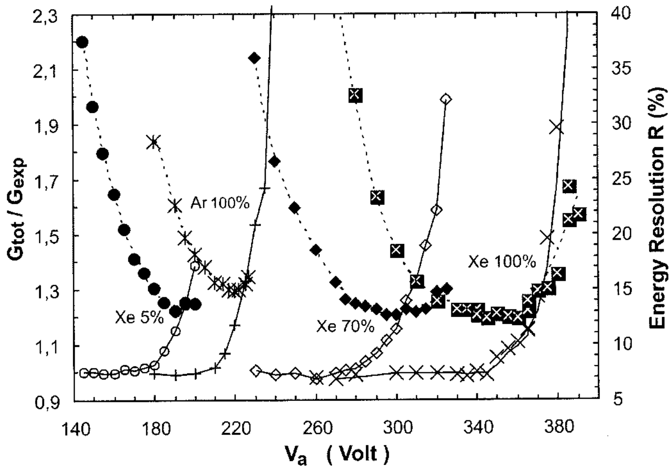

Fig. 4. Positive feedback gain (open symbols) and detector energy resolution (full symbols) as a function of the anode-to-cathode strip voltage V_a for constant reduced electric fields in the drift and scintillation regions and for the different argon–xenon mixture fillings. The solid lines serve only as a guide to the eye.

olution and relative gain due to positive feedback $G_{\rm tot}/G_{\rm exp}$ (where $G_{\rm tot}$ is the measured total gain of the detector and $G_{\rm exp}$ is the gain represented by the exponential function; Fig.3) as a function of V_a. The solid lines serve only as a guide to the eye. The data sets for Ar–10% Xe and Ar–20% Xe are not depicted since their relative gains overlap that of pure argon.

For all the mixtures, the detector energy resolution improves with the MSP gain, degrading after the onset of the positive feedback effect. Best energy resolutions are achieved for positive feedback gains of about 1.1, corresponding to V_a voltages of about 220, 190, 210, 220, 300, and 360 V for pure argon, Ar–5% Xe, Ar–10% Xe, Ar–20% Xe, Ar–70% Xe, and pure xenon, respectively. On the other hand, the use of reduced gains at the optimum operating conditions of the MSP results in a negligible charge buildup and prevents the possibility of MSP discharge breakdown.

The detector relative pulse amplitude and energy resolution were studied as a function of the reduced electric field E/p (the electric field intensity divided by the gas pressure p) in the scintillation region. However, the maximum achievable E/p was restrained due to insulation problems between the detector radiation window and the G1 holder and depended on the gas mixture, being about 5.5, 3.5, 4.0, 4.6, 5.5, and 6.5 V·cm^{-1}·Torr^{-1} for pure argon, Ar–5% Xe, Ar–10% Xe, Ar–20% Xe, Ar–70% Xe, and pure xenon, respectively.

Fig. 5 depicts the detector relative pulse amplitude and energy resolution as a function of the reduced electric field E/p in the scintillation region for the different argon–xenon mixtures, while keeping the reduced electric field constant in the drift region (at 0.3 V·cm^{-1}·Torr^{-1}) as well as the photosensor gain (at optimum value for each mixture). The solid curves serve only as a guide to the eye. The experimental results reveal the approximately linear trend above about 1 V·cm^{-1}·Torr^{-1} characteristic of the GPSC secondary scintillation yield. Below the gas scintillation threshold, pulse amplitudes become constant, the pulse height resulting only from the amplification of primary electrons in the MSP anodes.

In the region of high E/p, different behaviors are observed for the different mixtures. For pure xenon and high-Xe-content mixtures, the detector pulses tend to saturate. This effect can be explained considering the electric field intensity at the CsI surface and its role in the extraction of the produced photoelectrons. The increase of E/p in the scintillation region results in a decrease of the electric field intensity at the CsI surface. Consequently, an increase of E/p in the scintillation region may not lead to an increase of the detected photoelectrons because of the strong dependence of the photoelectron collection efficiency on the electric field at the CsI surface in xenon atmosphere [7]. Since this dependence is not significant for high-Ar-content mixtures and for CsI irradiation with 185-nm VUV photons [8], the increase of E/p in the scintillation region will not have a significant effect on the photoelectron collection efficiency and the detector pulse amplitude follows the characteristic exponential trend of the GPSC secondary scintillation above the gas ionization threshold.

Fig. 5 shows the advantages of the hybrid detector with Ar–Xe mixture fillings over those with pure Ar- or pure Xe-filling. Data sets for 5% Xe and 10% Xe overlap that of 20% Xe. The amplification achieved in the scintillation processes for Ar–Xe mixtures can reach values 50% higher than those obtained for pure argon or pure xenon. Additionally, detector energy resolutions obtained with Ar–Xe mixtures are better than those obtained with pure Ar- or pure Xe-filling. Extrapolating the results depicted in Fig. 5 for Ar–Xe mixtures to higher values of E/p, we estimated that values between 15–18 and between 11–10% can be obtained for light amplification and energy resolution, respectively, prior to the onset of the degrading effects from the presence of charge multiplication in the scintillation region [4], [16]. The achieved improvements result from the higher photoelectron collection efficiency of the photoelectrons emitted by the CsI-photocathode operating in Ar–Xe mixtures when compared to pure xenon, and from the more favorable wavelength scintillation emitted by these mixtures (172 nm) when compared to that of pure argon (128 nm) [9]–[11].

Xenon concentrations around 20% may produce somewhat higher light amplifications and slightly better energy resolutions. However, Xe concentrations as high as 70%, which have higher X-ray detection efficiency, can achieve about the same performance at higher reduced electric fields in the scintillation region.

IV. Conclusion

GPSC/MSGC hybrid detectors filled with argon–xenon mixtures present superior performance when compared to those with pure argon and pure xenon fillings. For these mixtures, the signal amplification due to the scintillation processes and the detector energy resolution may achieve values of 15%–18% and 11%–10%, respectively. This improvement in the energy resolutions can be achieved for mixtures with a broad range of xenon concentration, 20%–70% Xe, being achieved for lower reduced electric fields in the scintillation region as the xenon concentration is reduced.

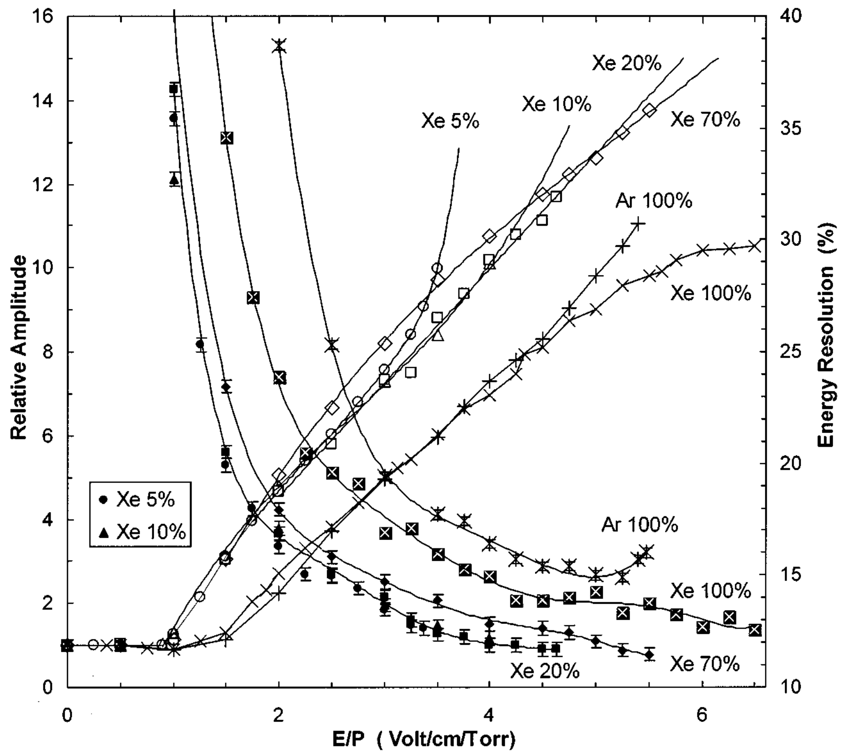

Fig. 5. Detector relative pulse amplitude (open symbols) and energy resolution (full symbols) as a function of the reduced electric field in the scintillation region for the different mixtures using a constant photosensor gain (at optimum value for each mixture) and a constant reduced electric field in the drift region (0.3 $V{\cdot}cm^{-1}{\cdot}Torr^{-1}$). The solid curves serve only as a guide to the eye.

As for pure argon or pure xenon filling, the detector performance is limited by optical positive feedback resulting from additional scintillation produced in the electron avalanche processes around the MSP anodes, limiting the MSP gain for optimum operating conditions. Best energy resolutions are achieved for positive feedback gains of about 1.1, corresponding to V_a voltages of about 220, 190, 210, 220, 300, and 360 V for pure argon, Ar-5% Xe, Ar-10% Xe, Ar-20% Xe, Ar-70% Xe, and pure xenon, respectively.

REFERENCES

[1] K. Zeitelhack, J. Friese, R. Gernhäuser, P. Kienle, H.-J. Körner, P. Maier-Komor, and S. Winkler, "A microstrip gas counter for single VUV photons," *Nucl. Instrum. Methods*, vol. A351, pp. 585–587, 1994.

[2] J. F. C. A. Veloso, J. A. M. Lopes, J. M. F. dos Santos, and C. A. N. Conde, "A microstrip gas chamber as a VUV photosensor for a xenon gas proportional scintillation," *IEEE Trans. Nucl. Sci.*, vol. 43, pp. 1232–1236, 1996.

[3] J. F. C. A. Veloso, J. M. F. dos Santos, and C. A. N. Conde, "Performance characteristics of a gas proportional scintillation counter coupled to a microstrip gas chamber photosensor," *Nucl. Instrum. Methods*, vol. A422, pp. 273–277, 1999.

[4] ——, "Gas proportional scintillation counter with a CsI-covered microstrip plate UV photosensor for high resolution x-ray spectrometry," *Nucl. Instrum. Methods*, vol. A457, pp. 253–261, 2001.

[5] J. F. C. A. Veloso, J. M. F. dos Santos, C. A. N. Conde, F. Mulhauser, P. Knowles, C. Donche-Gay, O. Huot, D. Taqqu, and F. Kottmann, "Driftless gas proportional scintillation counter for muonic hydrogen X-ray spectroscopy under strong magnetic fields," *Nucl. Instrum. Methods*, vol. A460, pp. 297–305, 2001.

[6] D. S. A. P. Freitas, J. F. C. A. Veloso, J. M. F. dos Santos, and C. A. N. Conde, "A comparative study of microstrip plate geometries as UV photosensors with reflective photocathodes: simulation," *IEEE Trans. Nucl. Sci.*, vol. 48, pp. 411–416, 2001.

[7] P. J. B. M. Rachinhas, J. A. M. Lopes, T. H. V. T. Dias, F. P. Santos, C. A. N. Conde, and A. D. Stauffer, "Photoelectron collection efficiency in rare gases: A Monte Carlo study," in *Proceedings of MC2000—International Conference on Advanced Monte Carlo for Radiation Physics, Particle Simulation and Applications*, M. Nakagawa, P. Vaz, F. Barão, A. Kling, and L. Távora, Eds. Heidelberg: Springer-Verlag, 2001, pp. 535–542.

[8] A. Buzulutskov, L. Shekhtman, A. Bressan, A. Di Mauro, L. Ropelewski, F. Sauli, and S. F. Biaggi, "GEM operation in pure noble gases and the avalanche confinement," *Nucl. Instrum. Methods*, vol. A433, pp. 471–475, 1999.

[9] C. M. B. Monteiro, J. F. C. A. Veloso, D. S. A. P. Freitas, J. M. F. dos Santos, and C. A. N. Conde, "The gas proportional scintillation counter/microstrip gas chamber hybrid detector with argon filling," Nucl. Instrum. Methods, vol. A, submitted for publication.

[10] A. Akkerman, T. Boutboul, A. Breskin, R. Chechik, and A. Gibrekhterman, "Low-energy electron transport in alkali-halides," *J. Appl. Phys.*, vol. 76, pp. 4656–4662, 1994.

[11] T. H. Di Stefano and W. E. Spicer, "Photoemission from CsI: Experiment," *Phys. Rev. B*, vol. 7, pp. 1554–1563, 1973.

[12] D. F. Anderson, "Properties of CsI and CsI-TMAE photocathodes," *Nucl. Instrum. Methods*, vol. A323, pp. 626–634, 1992.

[13] A. Breskin, A. Buzulutskov, and R. Chechik, "New ideas in CsI-based photondetectors: Wire photomultipliers and protection of the photocathodes," *IEEE Trans. Nucl. Sci.*, vol. 42, pp. 298–305, 1995.

[14] J. Va'vra, A. Breskin, A. Buzulutskov, R. Chechik, and E. Shefer, "Study of CsI photocathodes: Volume resistivity and aging," *Nucl. Instrum. Methods*, vol. A 387, pp. 154–162, 1997.

[15] R. Bouclier, M. Capeans, G. Million, L. Ropelewski, F. Sauli, T. Temmel, G. Della Mea, G. Maggioni, and V. Rigato, "High rate operation of micro-strip gas chambers on diamond-coated glass," *Nucl. Instrum. Methods*, vol. A 369, pp. 328–331, 1996.

[16] F. I. G. M. Borges, J. M. F. dos Santos, T. H. V. T. Dias, F. P. Santos, P. J. B. M. Rachinhas, and C. A. N. Conde, "Operation of gas proportional scintillation counters in a low charge multiplication regime," *Nucl. Instrum. Methods*, vol. A422, pp. 321–325, 1999.